Letter

Electronic states dressed by an out-of-plane supermodulation in the quasi-two-dimensional kagome superconductor CsV_3Sb_5

Yang Luo,[1,*] Shuting Peng,[1,*] Samuel M. L. Teicher,[2,*] Linwei Huai,[1,*] Yong Hu,[1,3] Yulei Han,[4,1] Brenden R. Ortiz,[2] Zuowei Liang,[1] Zhiyuan Wei,[1] Jianchang Shen,[1] Zhipeng Ou,[1] Bingqian Wang,[1] Yu Miao,[1] Mingyao Guo,[1] Makoto Hashimoto,[5] Donghui Lu,[5] Zhenhua Qiao,[1] Zhenyu Wang,[1,†] Stephen D. Wilson,[2,‡] Xianhui Chen,[1] and Junfeng He[1,§]

[1]*Department of Physics and CAS Key Laboratory of Strongly-coupled Quantum Matter Physics, University of Science and Technology of China, Hefei, Anhui 230026, China*

[2]*Materials Department and California Nanosystems Institute, University of California Santa Barbara, Santa Barbara, California 93106, USA*

[3]*Swiss Light Source, Paul Scherrer Institute, CH-5232 Villigen PSI, Switzerland*

[4]*Department of Physics, Fuzhou University, Fuzhou, Fujian 350108, China*

[5]*Stanford Synchrotron Radiation Lightsource, SLAC National Accelerator Laboratory, Menlo Park, California 94025, USA*

(Received 13 December 2021; revised 13 May 2022; accepted 18 May 2022; published 21 June 2022)

CsV_3Sb_5 has attracted much recent attention as the first quasi-two-dimensional (2D) kagome superconductor. While the kagome layers are 2D in nature, increasing evidence has pointed to the importance of out-of-plane correlation in this material. However, it remains unclear whether such correlation can change the fundamental electronic structure of the quasi-2D system. Here, we reveal this missing piece of information, using angle-resolved photoemission spectroscopy, complemented by scanning tunneling microscope measurements. The three-dimensional electronic structures in the high-temperature state are revealed, which agree well with density-functional theory calculations. Electron energy bands are observed in the low-temperature state that exhibit additional periodicities along the out-of-plane momentum. These results reveal a direct response to the out-of-plane electronic supermodulation in the single-particle spectral function of CsV_3Sb_5, thus establishing an electronic platform to examine emergent phenomena beyond 2D limit in kagome superconductors.

DOI: 10.1103/PhysRevB.105.L241111

The physical properties of layered materials are primarily 2D, but some rare phenomena may appear when the appropriate out-of-plane correlation is turned on, which could interact with both bulk and surface states of the material. Recently, a layered kagome material, CsV_3Sb_5, has attracted much attention as the first member of a new class of AV_3Sb_5 (A = K, Rb, Cs) kagome superconductors [1–44]. As shown in Fig. 1(a), CsV_3Sb_5 has a typical layered crystal structure [Fig. 1(a)]. The V sublattice forms a perfect kagome net [Fig. 1(b), which is interwoven with a hexagonal net of Sb atoms in the same plane [Fig. 1(a)]. This V_3Sb layer is then bounded above and below by Sb honeycomb lattices and Cs hexagonal lattices. While topologically nontrivial states and electron correlation effects are naturally expected from the 2D kagome layers, the existence of 3D charge-density wave (CDW) orders ($T_{CDW} = 94$ K) [4–7], a bulk superconducting state ($T_c = 2.5$ K) [9], and interlayer-interaction-driven broken symmetries [2,3,10,11], points to the importance of out-of-plane correlation in this material system.

In this paper, we report systematic studies on the evolution of the 3D electronic structure in CsV_3Sb_5 (see Supplemental Material for experimental details [45]; see also Refs. [8,9,46–48] therein). The 3D electron energy bands in the high-temperature state have been measured, which are consistent with the density-functional theory (DFT) calculations. However, bands are revealed at a low temperature, which exhibit additional periodicities along the out-of-plane momentum (K_Z) beyond that of the crystal lattice. These results demonstrate the importance of the out-of-plane electronic supermodulation in CsV_3Sb_5, which directly changes the single-particle spectral function of the material. Possible origins of the corresponding out-of-plane electronic supermodulation are discussed.

We first examine the 3D electronic structure of CsV_3Sb_5 in the high-temperature normal state without any electronic orders. The 3D Brillouin zone (BZ) and the projected in-plane BZ of CsV_3Sb_5 are presented in Fig. 1(c). For clarity, we use $\Gamma(A)$, $K(H)$, and $M(L)$ to mark the specific momentum points in the 3D BZ, and use $\bar{\Gamma}$, $\bar{K}$ and $\bar{M}$ to denote the momentum region only defined by the in-plane momentum, hereafter. DFT calculations along the high-symmetry directions in the 3D Brillouin zone are shown in Fig. 1(d). The most prominent features along the out-of-plane direction are seen in the band structure near Γ and A points. The electron-like band around Γ (marked in red) is much shallower than

*These authors contributed equally to this work.
†zywang2@ustc.edu.cn
‡stephendwilson@ucsb.edu
§jfhe@ustc.edu.cn

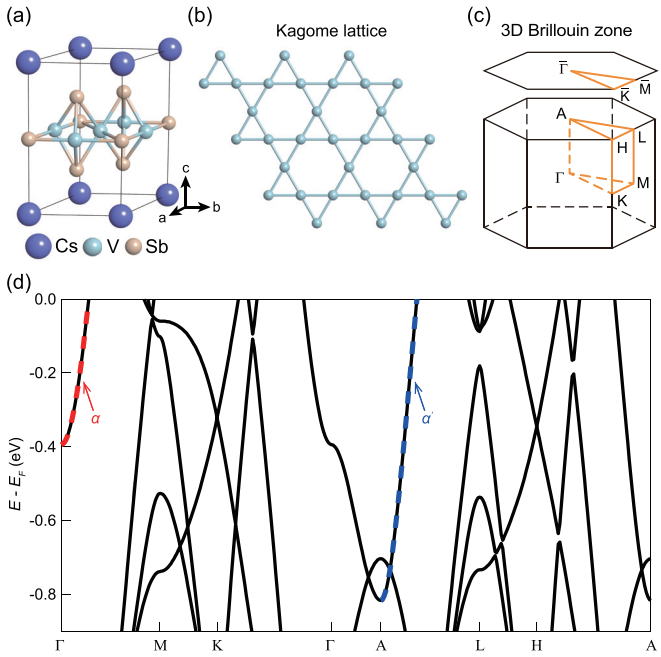

FIG. 1. Calculated 3D electronic structure of CsV_3Sb_5 in the high-temperature normal state. (a) Crystal structure of CsV_3Sb_5. (b) The kagome lattice formed by vanadium atoms. (c) Schematic of the 3D BZ and the projected in-plane BZ. (d) DFT band structure along the high-symmetry directions in the 3D BZ. The red (blue) dashed line marks the $\alpha(\alpha')$ band around Γ (A) point.

that around A (marked in blue). As such, the band bottom at Γ is closer to the Fermi level (E_F), comparing to that at A point. For simplicity, we label these two bands as α and α' hereafter [Fig. 1(d)]. Angle-resolved photoemission spectroscopy (ARPES) measurements have been carried out at 200 K ($T \gg T_{\mathrm{CDW}}$) with different photon energies (Fig. 2). The electron-like band at the zone center shows a clear photon energy dependence [Figs. 2(a)–2(c)]. While a moderate broadening of the band is seen at selected photon energies, which has been suggested as either K_Z broadening [12] or quantum well states on the surface [13], an overall periodic evolution of the band as a function of the out-of-plane momentum can be unambiguously identified [Figs. 2(c)–2(d)]. As shown in Figs. 2(a)–2(c), the bottom of the electron-like band reaches a minimum binding energy (absolute value of E-E_F) at Γ and a maximum binding energy at A, which is consistent with that of the α and α' bands in the DFT calculations. We note that the absolute energies for the band bottom are slightly different between the experiments and the calculations. This could be related to the surface potential which is not included in the DFT calculations, or due to some small uncertainties on the lattice parameters used in the calculations. Nevertheless, an overall agreement is achieved between the measured and calculated 3D electronic structure in the high-temperature normal state of CsV_3Sb_5.

Next, we study the electronic structure of CsV_3Sb_5 in the low-temperature state. ARPES measurement at 25 K across the Γ point reveals a double-band feature [Fig. 3(a)], which is different from the single electron-like band around Γ in the high-temperature state [Fig. 3(c)]. A careful examination of the low-temperature momentum distribution curves (MDCs) confirms the appearance of an electron-like band [marked by the blue triangles in Fig. 3(b)] in addition to the original α band (marked by the red triangles in Figs. 3(b) and 3(d); also see Supplemental Fig. S1 [45]). This is also clearly seen in energy distribution curves (EDCs) [Fig. 3(e)]. Comparing to the α band, this other band is weaker in photoemission intensity, but much deeper in energy [Figs. 3(a) and 3(e)]. Its bandwidth and overall dispersion are similar to the α' band around the A point in the high-temperature state. However, this well-separated double-band feature disappears along a momentum cut near the middle point between Γ and A in the BZ (cut 2 in Fig. 3(i)]. As shown in Fig. 3(f), hints of two bands may still be discernible along this cut, but these two electron-like bands are nearly degenerate in energy. Moreover, the bottom of the degenerate bands is now between that of α and α' bands in the high-temperature state [Figs. 3(e) and 3(f)]. Surprisingly, the double-band feature appears again along a momentum cut near the A point [Fig. 3(g); cut 3 in Fig. 3(i)]. The overall dispersion and bottoms of the two bands are similar to those observed near Γ, mimicking the α and α bands in the high-temperature states. But, the relative intensity of the two bands is swapped, and the low-energy band (α band) becomes much weaker. Then, the double-band feature changes into degenerate bands again, when the momentum cut is further moved up to a location near the middle point between A and Γ in the next BZ [Fig. 3(h); cut 4 in Fig. 3(i)]. These results indicate another periodicity of BZ/2 along the out-of-plane direction. This periodicity of the double-band feature as well as the swapped intensity between the two bands are more clearly visualized by the systematic photon-energy dependent (K_z-dependent) measurements of the EDC at $K_x = 0$ [across the band bottom; Fig. 3(j)].

After revealing the low-temperature band reconstruction (also see Supplemental Fig. S2 [45]), we move to discuss the possible origin. First, the coexistence of two bands at low temperature seems to suggest a band splitting, which has been reported in magnetic material systems [49] and materials with surface quantum-well states [13,50]. However, CsV_3Sb_5 does not exhibit any resolvable magnetic order [9], and 2D band splitting cannot give rise to the out-of-plane momentum-dependent band reconstruction observed in the low-temperature measurements. Electron-phonon coupling can also give rise to a replica band at a deeper energy [51]. But, the energy separation between the two bands at Γ is $\sim$300 meV, which is much higher than the phonon energies in CsV_3Sb_5. A band folding along the out-of-plane direction may work better to explain the experimental observations. If we consider an electronic supermodulation with an out-of-plane wave vector connecting Γ and A [Q1 in Fig. 4(b)], then the unit cell is doubled, and the ΓMK plane in the BZ will be folded to the ALH plane. As such, the α band along M-Γ-M will be folded to the L-A-L direction, and the α' band along L-A-L will also be folded to the M-Γ-M direction, giving rise to the double-band feature observed at both Γ and A in the experiment [Fig. 4(a)]. When the momentum cut is close to the middle point between Γ and A in the BZ, the folded band has almost the same K_Z as that of the original band.

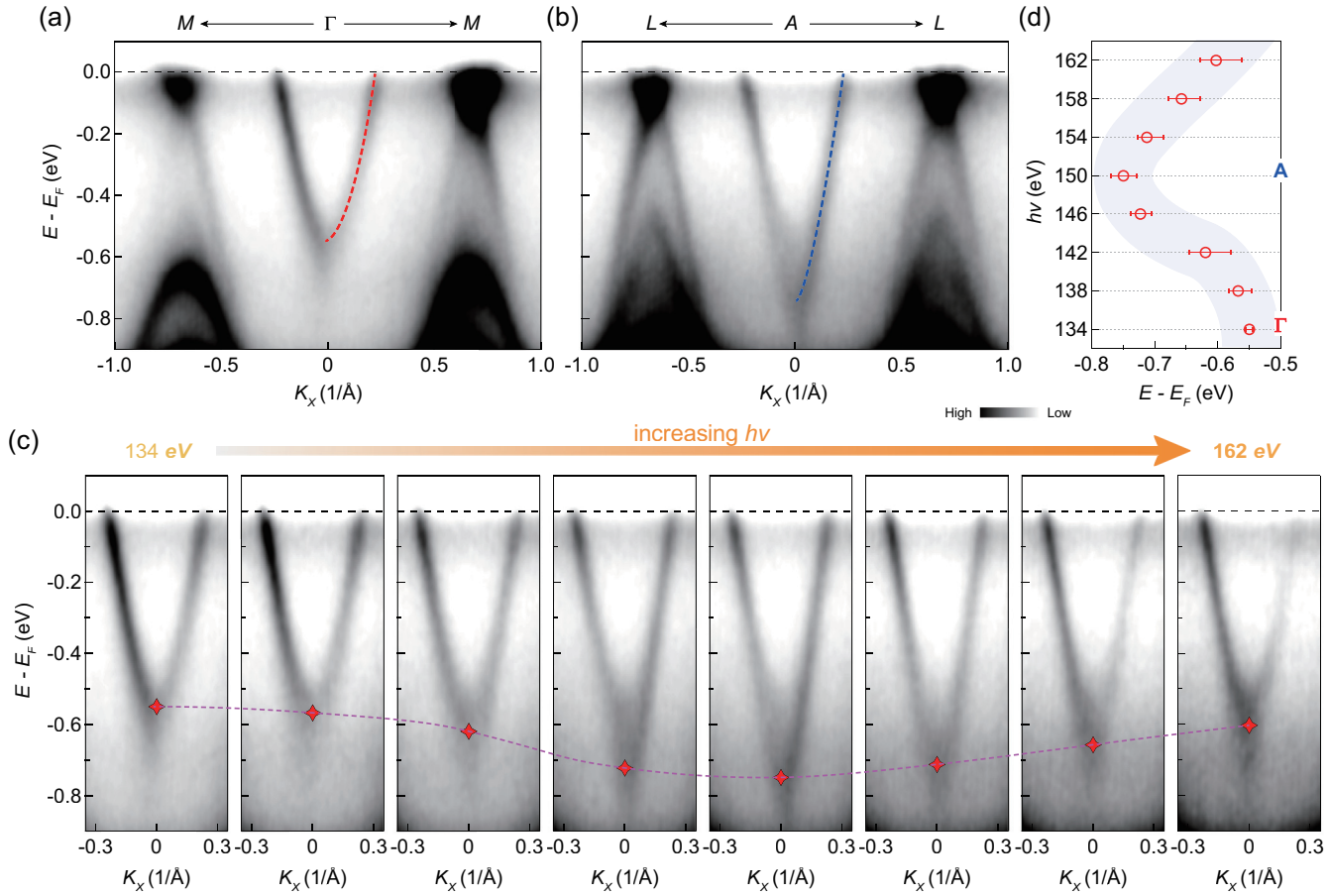

FIG. 2. The measured 3D electronic structure of CsV_3Sb_5 in the high-temperature normal state ($T = 200$ K). (a), (b) Photoelectron intensity plots along M-Γ-M (a) and L-A-L (b), measured with 134- and 150-eV photons, respectively. (c) The electron-like band as a function of photon energies. The red diamonds mark the evolution of the band bottom. The pink dashed line is a guide to the eye. (d) The energy of the band bottom as a function of photon energies, extracted from (c). The error bars are from the uncertainties in the determination of the band-bottom position. The measurements have been carried out with circularly polarized light.

Thus, two nearly degenerate bands are observed. This scenario also explains the swapped intensity between the two bands as a function of K_z at $\bar{\Gamma}$ [Fig. 3(j)] because photoemission intensity of a folded band (FB) is in general weaker than that of the original main band (MB), and the main band changes from α band at Γ to α' band at A in the measurements [Fig. 3(j)]. Since the out-of-plane band folding has well explained the low-temperature electronic structure at $\bar{\Gamma}$, it would be interesting to check whether the band folding is also at work near the $\bar{M}$ region. We note that a low-temperature double-band feature is indeed discernible at M, although it is relatively weak (see Supplemental Fig. S3 [45]; see, also, Ref. [52] therein). Nevertheless, the band reconstruction at $\bar{M}$ is more complicated than that at $\bar{\Gamma}$, because the in-plane CDW order (2×2) has been reported to show a significant effect on the band structure near $\bar{M}$ beyond a direct band folding [27,41].

The last issue to discuss is the origin of the electronic supermodulation that accounts for the out-of-plane band folding. STM measurements and real-space resolved photoemission experiments have been carried out. Our STM results reveal two types of surface regions on the cleaved sample: one is mainly terminated with Cs atoms [Cs-rich region, Fig. 4(d)], and the other is primarily covered with Sb atoms [Cs-deficient region, Fig. 4(e)]. The real-space resolved photoemission measurements demonstrate that the low-temperature out-of-plane band reconstruction mainly takes place on the Cs-rich region, evidenced by the strong Cs peak in the core-level measurements [Fig. 4(c)]. On the contrary, the band reconstruction becomes less clear on the Cs-deficient region (Supplemental Fig. S4 [45]). These results seem to suggest that the band reconstruction is related to the Cs atoms on the surface. Then, the first candidates to consider about are the surface states of the Cs atoms and the surface reconstructions associated with Cs atoms. However, both surface states and surface reconstructions are 2D, which cannot give rise to the out-of-plane electronic supermodulation (see Supplemental Figs. S5 and S6 [45]; see, also, Refs. [54,55] therein). Another potential candidate is the 3D CDW reported in CsV_3Sb_5 [4–7,29], which can provide the out-of-plane scattering channel below the CDW transition temperature. This seems to be consistent with the band folding at low temperature (Supplemental

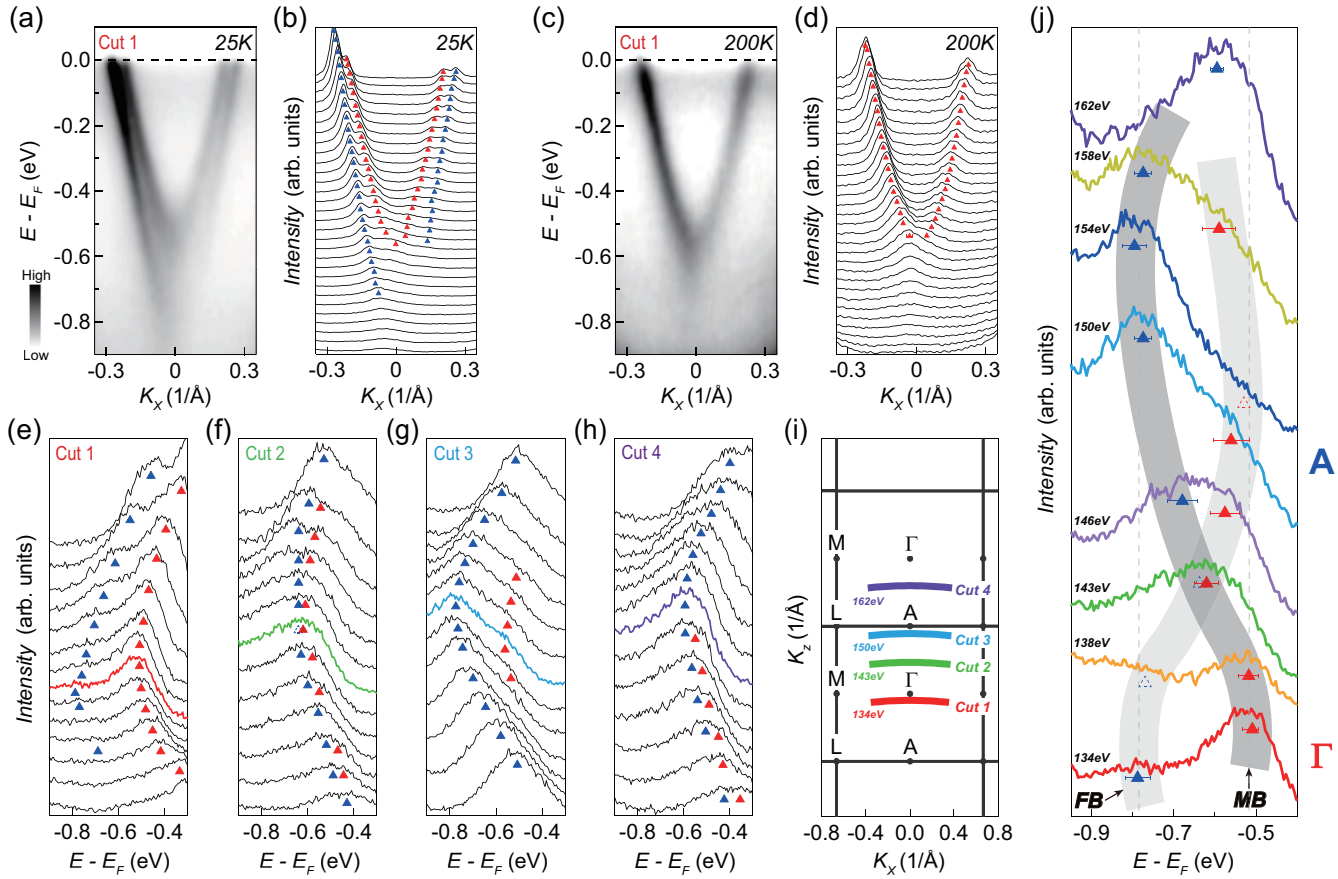

FIG. 3. Low-temperature band reconstruction near $\bar{\Gamma}$. (a), (b) Photoelectron intensity plot (a) and MDCs (b) near Γ [cut 1 in (i)] measured at 25 K. The red and blue triangles mark the peaks for the two electron-like bands, respectively. (c), (d) Same as (a), (b), but measured at 200 K. (e)–(h) Photoelectron raw spectra (EDCs) measured along cut 1, cut 2, cut 3 and cut 4, respectively. The locations of the momentum cuts are shown in (i). (j) EDC at $K_X = 0$ (across the band bottom) as a function of the out-of-plane momentum. The measurements have been carried out with circularly polarized light and the corresponding photon energies are noted. The red (blue) triangles mark the peaks with a smaller (larger) binding energy. The dark (light) gray belt is a guide to the eye for the main (folded) band.

Fig. S2 [45]), as well as our STM results which reveal the characteristic modulation for the 3D CDW order on the Cs termination [Fig. 4(d)]. However, this scenario might not explain the less clear band reconstruction on the Cs-deficient region, since the 3D CDW order can also be seen on the Sb termination [2]. Nevertheless, we note that the electronic structures on the Sb termination would be more complicated, which are affected by a combined effect of both the 3D CDW order and another interesting 4×1 CDW order [2]. If the 3D CDW scenario works, then the reported $(2 \times 2 \times 2)$ CDW order would give rise to the scattering wave vector (Q1) that accounts for the other out-of-plane periodicity of BZ/2 observed at $\bar{\Gamma}$ [Fig. 4(b)]. In the meantime, another $(2 \times 2 \times 4)$ CDW order has been observed by x-ray diffraction [6], which would provide a smaller scattering wave vector [Q2, Fig. 4(b)]. It remains to be explored whether a BZ/4 periodicity can be further identified in the electronic structure. The last possibility is the existence of an out-of-plane order near the Cs surface, which reconstructs the out-of-plane electronic structure. In principle, the electronic states near $\bar{\Gamma}$ are dominated by Sb Pz orbital [29,37] (see Supplemental Fig. S7 [45]), which is presumably more sensitive to out-of-plane correlation near the surface layers, whereas the V d orbitals at $\bar{M}$ might be influenced by the order that is more long range in the bulk [6]. Future work would be stimulated to explore whether such a hidden order [56] could appear in the low-temperature state of CsV_3Sb_5, and whether the few layers near the Cs surface would be affected. If yes, it would be interesting to investigate whether this near-surface out-of-plane order also interacts with the topological surface states in this material system [9,27].

In summary, our work reveals the 3D electronic structure of CsV_3Sb_5 in the high-temperature normal state and unveils a direct coupling of an out-of-plane electronic supermodulation to the single-particle spectral function at low temperature. We note that electronic states dressed by the out-of-plane correlation in CsV_3Sb_5 may have important implications. For instance, high-temperature superconductivity in cuprates shows 3D superconducting coherence with primarily 2D copper-oxygen planes [57,58]. The experimental identification of 3D charge order in cuprates reveals an intimate link between superconductivity and charge order beyond

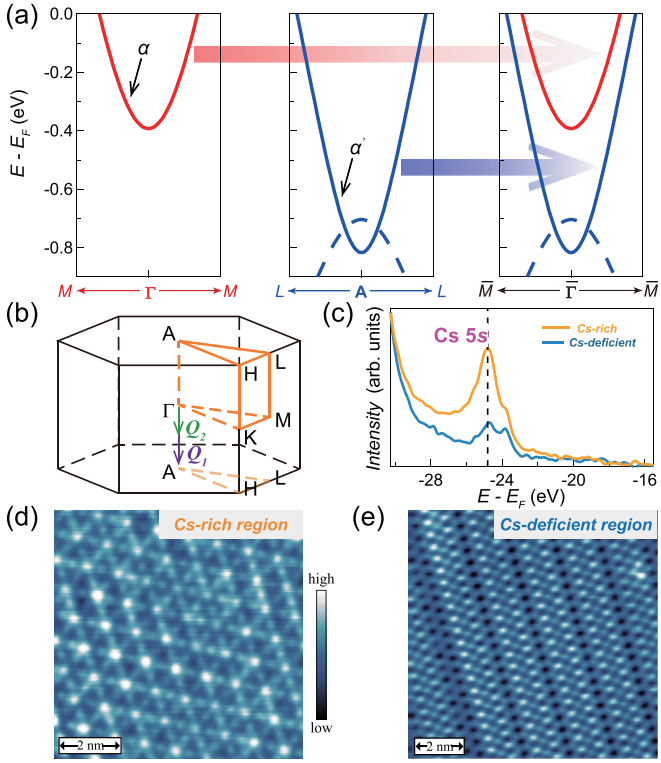

FIG. 4. Out-of-plane band folding. (a) Folding of the DFT bands along the out-of-plane direction. The $\alpha(\alpha')$ band around Γ (A) point is shown in red (blue). The blue dashed line indicates a holelike band close to the bottom of the α' band in the DFT calculation. However, this band disappears when in-plane component of the charge order [27] or electron correlation [53] is considered in the calculation. (b) Schematic of the scattering process along the out-of-plane direction. (c) Photoemission core-level measurements on the Cs-rich and Cs-deficient regions, respectively. (d) STM measurement on the Cs-rich region. (e) Same as (d), but on the Cs-deficient region. The STM setup conditions are $V_s = 20\,\mathrm{mV}$, $I_t = 780\,\mathrm{pA}$, $T = 4.8\,\mathrm{K}$ in (d), and $V_s = -100\,\mathrm{mV}$, $I_t = 140\,\mathrm{pA}$, $T = 4.8\,\mathrm{K}$ in (e).

simple competition [59]. In quasi-2D kagome metals, the existence of 3D superconductivity is rare. It is first realized in CsV_3Sb_5, where the out-of-plane electronic supermodulation also appears and dresses the quasi-2D electronic structure. It would be interesting to explore the nature of the out-of-plane interaction that stabilizes the 3D ordering tendencies in CsV_3Sb_5 and other quasi-2D kagome superconductors.

ACKNOWLEDGMENTS

We thank useful discussions with M. Shi, T. Wu, J.-J. Ying, and Z.-J. Xiang. The work at University of Science and Technology of China (USTC) was supported by the Fundamental Research Funds for the Central Universities (Grants No. WK3510000008 and No. WK3510000012) and USTC start-up fund. The work at UC Santa Barbara was supported via the UC Santa Barbara NSF Quantum Foundry funded via the Q-AMASE-i program under Award No. DMR-1906325. This research made use of the shared facilities of the NSF Materials Research Science and Engineering Center at UC Santa Barbara (Grant No. DMR-1720256). The UC Santa Barbara MRSEC is a member of the Materials Research Facilities Network [60]. S.M.L.T. acknowledges use of the shared computing facilities of the Center for Scientific Computing at UC Santa Barbara, supported by NSF Grant No. CNS-1725797 and NSF Grant No. DMR-1720256. B.R.O. acknowledges support from the California NanoSystems Institute through the Elings Fellowship program. S.M.L.T has been supported by the National Science Foundation Graduate Research Fellowship Program under Grant No. DGE-1650114. The work at PSI was supported by the Swiss National Science Foundation under Grant. No. 200021-188413, and the Sino-Swiss Science and Technology Cooperation (Grant No. IZLCZ2-170075). Use of the Stanford Synchrotron Radiation Lightsource, SLAC National Accelerator Laboratory, is supported by the U.S. Department of Energy, Office of Science, Office of Basic Energy Sciences under Contract No. DE-AC02-76SF00515.

[1] F. H. Yu, D. H. Ma, W. Z. Zhuo, S. Q. Liu, X. K. Wen, B. Lei, J. J. Ying, and X. H. Chen, Unusual competition of superconductivity and charge-density-wave state in a compressed topological kagome metal, Nat. Commun **12**, 3645 (2021).

[2] H. Zhao, H. Li, B. R. Ortiz, S. M. L. Teicher, T. Park, M. Ye, Z. Wang, L. Balents, S. D.Wilson, and I. Zeljkovic, Cascade of correlated electron states in the kagome superconductor CsV_3Sb_5, Nature (London) **599**, 216 (2021).

[3] H. Chen, H. Yang, B. Hu, Z. Zhao, J. Yuan, Y. Xing, G. Qian, Z. Huang, G. Li, Y. Ye, S. Ma, S. Ni, H. Zhang, Q. Yin, C. Gong, Z. Tu, H. Lei, H. Tan, S. Zhou, C. Shen, X. Dong, B. Yan, Z. Wang, and H.-J, Gao, Roton pair density wave in a strong-coupling kagome superconductor, Nature (London) **599**, 222 (2021).

[4] Z. Liang, X. Hou, F. Zhang, W. Ma, P. Wu, Z. Zhang, F. Yu, J.-J. Ying, K. Jiang, L. Shan, Z. Wang, and X.-H. Chen, Three-Dimensional Charge Density Wave and Surface-Dependent Vortex-Core States in a Kagome Superconductor CsV_3Sb_5, Phys. Rev. X **11**, 031026 (2021).

[5] H. Li, T. T. Zhang, T. Yilmaz, Y. Y. Pai, C. E. Marvinney, A. Said, Q. W. Yin, C. S. Gong, Z. J. Tu, E. Vescovo, C. S. Nelson, R. G. Moore, S. Murakami, H. C. Lei, H. N. Lee, B. J. Lawrie, and H. Miao, Observation of Unconventional Charge Density Wave without Acoustic Phonon Anomaly in Kagome Superconductors AV_3Sb_5 (A = Rb, Cs), Phys. Rev. X **11**, 031050 (2021).

[6] B. R. Ortiz, S. M. L. Teicher, L. Kautzsch, P. M. Sarte, N. Ratcliffe, J. Harter, J. P. C. Ruff, R. Seshadri, and S. D. Wilson, Fermi Surface Mapping and the Nature of Charge-Density-Wave Order in the Kagome Superconductor CsV_3Sb_5, Phys. Rev. X **11**, 041030 (2021).

[7] D. Song, L. Zheng, F. Yu, J. Li, L. Nie, M. Shan, D. Zhao, S. Li, B. Kang, Z. Wu, Y. Zhou, K. Sun, K. Liu, X. Luo, Z. Wang, J. Ying, X. Wan, T. Wu, and X. Chen, Orbital ordering and fluctuations in a kagome superconductor CsV3Sb5, Sci. China Phys. Mech. Astron. **65**, 247462 (2022).

[8] B. R. Ortiz, L. C. Gomes, J. R. Morey, M. Winiarski, M. Bordelon, J. S. Mangum, I. W. H. Oswald, J. A. Rodriguez-Rivera, J. R. Neilson, S. D. Wilson, E. Ertekin, T. M. McQueen, and E. S. Toberer, New kagome prototype materials: Discovery of KV_3Sb_5, RbV_3Sb_5, and CsV_3Sb_5, Phys. Rev. Mater. **3**, 094407 (2019).

[9] B. R. Ortiz, S. M. L. Teicher, Y. Hu, J. L. Zuo, P.M. Sarte, E.C. Schueller, A. M. M. Abeykoon, M. J. Krogstad, S. Rosenkranz, R. Osborn, R. Seshadri, L. Balents, J. He, and S. D. Wilson, CsV_3Sb_5 : A $\mathbb{Z}_2$ Topological Kagome Metal with a Superconducting Ground State, Phys. Rev. Lett. **125**, 247002 (2020).

[10] T. Park, M. Ye, and L. Balents, Electronic instabilities of kagome metals: Saddle points and Landau theory, Phys. Rev. B **104**, 035142 (2021).

[11] M. H. Christensen, T. Birol, B. M. Andersen, and R. M. Fernandes, Theory of the charge density wave in AV_3Sb_5 kagome metals, Phys. Rev. B **104**, 214513 (2021).

[12] K. Nakayama, Y. Li, T. Kato, M. Liu, Z. Wang, T. Takahashi, Y. Yao, and T. Sato, Multiple energy scales and anisotropic energy gap in the charge-density-wave phase of the kagome superconductor CsV_3Sb_5, Phys. Rev. B **104**, L161112 (2021).

[13] Y. Cai, Y. Wang, Z. Hao, Y. Liu, X.-M. Ma, Z. Shen, Z. Jiang, Y. Yang, W. Liu, Q. Jiang, Z. Liu, M. Ye, D. Shen, Z. Sun, J. Chen, L. Wang, C. Liu, J. Lin, J. Wang, B. Huang, J.-W. Mei, and C. Chen, Emergence of Quantum Confinement in Topological Kagome Superconductor CsV_3Sb_5 family, arXiv:2109.12778.

[14] S. Ni, S. Ma, Y. Zhang, J. Yuan, H. Yang, Z. Lu, N. Wang, J. Sun, Z. Zhao, D. Li, S. Liu, H. Zhang, H. Chen, K. Jin, J. Cheng, L. Yu, F. Zhou, X. Dong, J. Hu, H.-J. Gao, and Z. Zhao, Anisotropic superconducting properties of kagome metal CsV_3Sb_5, Chin. Phys. Lett. **38**, 057403 (2021).

[15] X. Chen, X. Zhan, X. Wang, J. Deng, X.-B. Liu, X. Chen, J.-G. Guo, and X. Chen, Highly robust reentrant superconductivity in CsV_3Sb_5 under pressure, Chin. Phys. Lett. **38**, 057402 (2021).

[16] C. C. Zhao, L. S. Wang, W. Xia, Q. W. Yin, J. M. Ni, Y. Y. Huang, C. P. Tu, Z. C. Tao, Z. J. Tu, C. S. Gong, H. C. Lei, Y. F. Guo, X. F. Yang, and S. Y. Li, Nodal superconductivity and superconducting domes in the topological Kagome metal CsV_3Sb_5, arXiv:2102.08356.

[17] K. Y. Chen, N. N. Wang, Q. W. Yin, Y. H. Gu, K. Jiang, Z. J. Tu, C. S. Gong, Y. Uwatoko, J. P. Sun, H. C. Lei, J. P. Hu, and J.-G. Cheng, Double Superconducting Dome and Triple Enhancement of Tc in the Kagome Superconductor CsV_3Sb_5 under High Pressure, Phys. Rev. Lett. **126**, 247001 (2021).

[18] W. Duan, Z. Nie, S. Luo, F. Yu, B. R. Ortiz, L. Yin, H. Su, F. Du, A. Wang, Y. Chen, X. Lu, J. Y, S. D. Wilson, X. Chen, Y. Song, and H. Yuan, Nodeless superconductivity in the kagome metal CsV_3Sb_5, Sci. China Phys. Mech. Astron. **64**, 107462 (2021).

[19] Z. Zhang, Z. Chen, Y. Zhou, Y. Yuan, S. Wang, J. Wang, H. Yang, C. An, L. Zhang, X. Zhu, Y. Zhou, X. Chen, J. Zhou, and Z. Yang, Pressure-induced reemergence of superconductivity in the topological kagome metal CsV_3Sb_5, Phys. Rev. B **103**, 224513 (2021).

[20] Y. Xiang, Q. Li, Y. Li, W. Xie, H. Yang, Z. Wang, Y. Yao, and H.-H. Wen, Twofold symmetry of c-axis resistivity in topological kagome superconductor CsV_3Sb_5 with in-plane rotating magnetic field, Nat. Commun. **12**, 6727 (2021).

[21] H.-S. Xu, Y.-J. Yan, R. Yin, W. Xia, S. Fang, Z. Chen, Y. Li, W. Yang, Y. Guo, and D.-L. Feng, Multiband Superconductivity with Sign-Preserving Order Parameter in Kagome Superconductor CsV_3Sb_5, Phys. Rev. Lett. **127**, 187004 (2021).

[22] Y. Song, T. Ying, X. Chen, X. Han, X. Wu, A. P. Schnyder, Y. Huang, J.-G. Guo, and X. Chen, Competition of Superconductivity and Charge Density Wave in Selective Oxidized CsV_3Sb_5 Thin Flakes, Phys. Rev. Lett. **127**, 237001 (2021).

[23] F. H. Yu, T. Wu, Z. Y. Wang, B. Lei, W. Z. Zhuo, J. J. Ying, and X. H. Chen, Concurrence of anomalous Hall effect and charge density wave in a superconducting topological kagome metal, Phys. Rev. B **104**, L041103 (2021).

[24] X. Zhou, Y. Li, X. Fan, J. Hao, Y. Dai, Z. Wang, Y. Yao, and H.-H. Wen, Origin of the charge density wave in the kagome metal CsV_3Sb_5 as revealed by optical spectroscopy, Phys. Rev. B **104**, L041101 (2021).

[25] C. Mu, Q. Yin, Z. Tu, C. Gong, H. Lei, Z. Li, and J. Luo, S-wave superconductivity in kagome metal CsV_3Sb_5 revealed by $^{121/123}$Sb NQR and ^{51}V NMR measurements, Chin. Phys. Lett. **38**, 077402 (2021).

[26] N. Ratcliff, L. Hallett, B. R. Ortiz, S. D. Wilson, and J. W. Harter, Coherent phonon spectroscopy and interlayer modulation of charge density wave order in the kagome metal CsV_3Sb_5, Phys. Rev. Mater. **5**, L111801 (2021).

[27] Y. Hu, S. M. L. Teicher, B. R. Ortiz, Y. Luo, S. Peng, L. Huai, J. Ma, N. C. Plumb, S. D. Wilson, J. He, and M. Shi, Topological surface states and flat bands in the kagome superconductor CsV_3Sb_5, Sci. Bull. **67**, 495 (2022).

[28] Z. Wang, Y.-X. Jiang, J.-X. Yin, Y. Li, G.-Y. Wang, H.-L. Huang, S. Shao, J. Liu, P. Zhu, N. Shumiya, Md S. Hossain, H. Liu, Y. Shi, J. Duan, X. Li, G. Chang, P. Dai, Z. Ye, G. Xu, Y. Wang, H. Zheng, J. Jia, M. Z. Hasan, and Y. Yao, Electronic nature of chiral charge order in the kagome superconductor CsV_3Sb_5, Phys. Rev. B **104**, 075148 (2021).

[29] H. Tan, Y. Liu, Z. Wang, and B. Yan, Charge Density Waves and Electronic Properties of Superconducting Kagome Metals, Phys. Rev. Lett. **127**, 046401 (2021).

[30] X. Feng, K. Jiang, Z. Wang, and J. Hu, Chiral flux phase in the kagome superconductor AV_3Sb_5, Sci. Bull. **66**, 1384 (2021).

[31] M. M. Denner, R. Thomale, and T. Neuoert, Analysis of Charge Order in the Kagome Metal AV_3Sb_5 (A = K, Rb, Cs), Phys. Rev. Lett. **127**, 217601 (2021).

[32] Y.-P. Lin and R. M. Nandkishore, Complex charge density waves at Van Hove singularity on hexagonal lattices: Haldane-model phase diagram and potential realization in kagome metals AV_3Sb_5 (A = K, Rb, Cs), Phys. Rev. B **104**, 045122 (2021).

[33] Z. Wang, S. Ma, Y. Zhang, H. Yang, Z. Zhao, Y. Ou, Y. Zhu, S. Ni, Z. Lu, H. Chen, K. Jiang, L. Yu, Y. Zhang, X. Dong, J. Hu, H.-J. Gao, and Z. Zhao, Distinctive momentum dependent charge-density-wave gap observed in CsV_3Sb_5 superconductor with topological Kagome lattice, arXiv:2104.05556.

[34] Y. Fu, N. Zhao, Z. Chen, Q. Yin, Z. Tu, C. Gong, C. Xi, X. Zhu, Y. Sun, K. Liu, and H. Lei, Quantum Transport Evidence of Topological Band Structures of Kagome Superconductor CsV_3Sb_5, Phys. Rev. Lett. **127**, 207002 (2021).

[35] E. Uykur, B. R. Ortiz, O. Iakutkina, M. Wenzel, S. D. Wilson, M. Dressel, and A. A. Tsirlin, Low-energy optical properties of the non-magnetic kagome metal CsV_3Sb_5, Phys. Rev. B **104**, 045130 (2021).

[36] M. Kang, S. Fang, J.-K. Kim, B. R. Ortiz, S. H. Ryu, J. Kim, J. Yoo, G. Sangiovanni, D. D. Sante, B.-G. Park, C. Jozwiak, A. Bostwick, E. Rotenberg, E. Kaxiras, S. D. Wilson, J.-H. Prak, and R. Comin, Twofold Van Hove singularity and origin of charge order in topological kagome superconductor CsV_3Sb_5, Nat. Phys. **18**, 301 (2022).

[37] Y. Hu, X. Wu, B. R. Ortiz, S. Ju, X. Han, J. Ma, N. C. Plumb, M. Radovic, R. Thomale, S. D. Wilson, A. P. Schnyder, and M. Shi, Rich nature of Van Hove singularities in kagome superconductor CsV_3Sb_5, Nat Commun. **13**, 2220 (2022).

[38] R. Lou, A. Fedorov, Q. Yin, A. Kuibarov, Z. Tu, C. Gong, E. F. Schwier, B. Buchner, H. Lei, and S. Borisenko, Charge-Density-Wave-Induced Peak-Dip-Hump Structure and the Multiband Superconductivity in a Kagome Superconductor CsV_3Sb_5, Phys. Rev. Lett. **128**, 036402 (2022).

[39] B. Q. Song, X. M. Kong, W. Xia, Q. W. Yin, C. P. Tu, C. C. Zhao, D. Z. Dai, K. Meng, Z. C. Tao, Z. J. Tu, C. S. Gong, H. C. Lei, Y. F. Guo, X. F. Yang, and S. Y. Li, Competing superconductivity and charge-density wave in kagome metal CsV_3Sb_5: Evidence from their evolutions with sample thickness, arXiv:2105.09248.

[40] Z. Liu, N. Zhao, Q. Yin, C. Gong, Z. Tu, M. Li, W. Song, Z. Liu, D. Shen, Y. Huang, K. Liu, H. Lei, and S. Wang, Charge-density-wave-induced Bands Renormalization and Energy Gaps in a Kagome Superconductor RbV_3Sb_5, Phys. Rev. X **11**, 041010 (2021).

[41] S. Cho, H. Ma, W. Xia, Y. Yang, Z. Liu, Z. Huang, Z. Jiang, X. Lu, J. Liu, Z. Liu, J. Li, J. Wang, Y. Liu, J. Jia, Y. Guo, J. Liu, and D. Shen, Emergence of New Van Hove Singularities in the Charge Density Wave State of a Topological Kagome Metal RbV_3Sb_5, Phys. Rev. Lett. **127**, 236401 (2021).

[42] S.-Y. Yang, Y. J. Wang, B. R. Ortiz, D. Liu, J. Gayles, E. Derunova, R. Gonzalez-Hernandez, L. Šmejkal, Y. Chen, S. S. P. Parkin, S. D.Wilson, E. S. Toberer, T. McQueen, and M. N. Ali, Giant, unconventional anomalous Hall effect in the metallic frustrated magnet candidate, KV_3Sb_5, Sci. Adv. **6**, eabb6003 (2020).

[43] H. Luo, Q. Gao, H. Liu, Y. Gu, D. Wu, C. Yi, J. Jia, S. Wu, X. Luo, Y. Xu, L. Zhao, Q. Wang, H. Mao, G. Liu. Z. Zhu, Y. Shi, K. Jiang, J. Hu, Z. Xu, and X. J. Zhou, Electronic nature of charge density wave and electron-phonon coupling in kagome superconductor KV_3Sb_5, Nat. Commun. **13**, 273 (2022).

[44] K. Jiang, T. Wu, J.-X. Yin, Z. Wang, M. Z. Hasan, S. D. Wilson, X. Chen, and J. Hu, Kagome superconductors AV_3Sb_5 (A = K, Rb, Cs), arXiv:2109.10809.

[45] See Supplemental Material at http://link.aps.org/supplemental/10.1103/PhysRevB.105.L241111 for details of experiments, theoretical calculations, and data fitting.

[46] G. Kresse and J. Hafner, *Ab initio* molecular-dynamics simulation of the liquid-metal–amorphous-semiconductor transition in germanium, Phys. Rev. B **49**, 14251 (1994).,

[47] G. Kresse and J. Furthmuller, Efficient iterative schemes for ab initio total-energy calculations using a plane-wave basis set, Phys. Rev. B **54**, 11169 (1996).

[48] G. Kresse and J. Furthmuller, Efficiency of *ab-initio* total energy calculations for metals and semiconductors using a plane-wave basis set, Comput. Mater. Sci. **6**, 15 (1996).

[49] S. Jang, R. Kealhofer, C. John, S. Doyle, J.-S. Hong, J. H. Shin, Q. Si, O. Erten, J. D. Denlinger, and J. G. Analytis, Direct visualization of coexisting channels of interaction in CeSb, Sci. Adv. **5**, eaat7158 (2019).

[50] N. Gauthier, J. A. Sobota, M. Hashimoto, H. Pfau, D.-H. Lu, E. D. Bauer, F. Ronning, P. S. Kirchmann, and Z.-X. Shen, Quantum-well states in fractured crystals of the heavy-fermion material $CeCoIn_5$, Phys. Rev. B **102**, 125111 (2020).

[51] J. J. Lee, F. T. Schmitt, R. G. Moore, S. Johnston, Y.-T. Cui, W. Li, M. Yi, Z. K. Liu, M. Hashimoto, Y. Zhang, D.-H. Lu, T. P. Devereaux, D.-H. Lee, and Z.-X. Shen, Interfacial mode coupling as the origin of the enhancement of Tc in FeSe films on $SrTiO_3$, Nature (London) **515**, 245 (2014).

[52] P. Zhang, P. Richard, T. Qian, Y. M. Xu, X. Dai, and H. Ding, A precise method for visualizing dispersive features in image plots, Rev. Sci. Instrum. **82**, 043712 (2011).

[53] J. Zhao, W. Wu, Y. Wang, and S. A. Yang, Electronic correlations in the normal state of kagome superconductor KV_3Sb_5, Phys. Rev. B **103**, L241117 (2021).

[54] Q. Wu, S. Zhang, H.-F. Song, M. Troyer, and A. A. Soluyanov, WannierTools: An open-source software package for novel topological materials, Comput. Phys. Commun. **224**, 405 (2018).

[55] M. Mende, K. Ali, G. Poelchen, S. Schulz, V. Mandic, A. V. Tarasov, C. Polley, A. Generalov, A. V. Fedorov, M. Güttler, C. Laubschat, K. Kliemt, Y. M. Koroteev, E. V. Chulkov, K. Kummer, C. Krellner, D. Y. Usachov, and D. V. Vyalikh, Strong Rashba effect and different $f-d$ hybridization phenomena at the surface of the heavy-fermion superconductor $CeIrIn_5$, Adv. Elec. Mater. **8**, 2100768 (2021).

[56] L. Zhao, D. H. Torchinsky, H. Chu, V. Ivanov, R. Lifshitz, R. Flint, T. Qi, G. Cao, and D. Hsieh, Evidence of an odd-parity hidden order in a spin–orbit coupled correlated iridate, Nat. Phys. **12**, 32 (2016).

[57] A. Damascelli, Z. Hussain, and Z. X. Shen, Angle-resolved photoemission studies of the cuprate superconductors, Rev. Mod. Phys. **75**, 473 (2003).

[58] M. Hepting, L. Chaix, E. W. Huang, R. Fumagalli, Y. Y. Peng, B. Moritz, K. Kummer, N. B. Brookes, W. C. Lee, M. Hashimoto, T. Sarkar, J.-F. He, C. R. Rotundu, Y. S. Lee, R. L. Greene, L. Braicovich, G. Ghiringhelli, Z. X. Shen, T. P. Devereaux, and W. S. Lee, Three-dimensional collective charge excitations in electron-doped copper oxide superconductors, Nature (London) **563**, 374 (2018).

[59] S. Gerber, H. Jang, H. Nojiri, S. Matsuzawa, H. Yasumura, D. A. Bonn, R. Liang, W. N. Hardy, Z. Islam, A. Mehta, S. Song, M. Sikorski, D. Stefanescu, Y. Feng, S. A. Kivelson, T. P. Devereaux, Z.-X. Shen, C.-C. Kao, W.-S. Lee, D. Zhu, and J.-S. Lee, Three-dimensional charge density wave order in $YBa_2Cu_3O_{6.67}$ at high magnetic fields, Science **350**, 949 (2015).

[60] www.mrfn.org.